Trace Metal Exposure from Dietary Supplements Differentially Inhibits Gram-Positive and Gram-Negative Bacterial Growth: Implications for Gut Microbial Homeostasis

Irene Sung[1], Sophia Kahng[2], Olivia Lee[3], Regina Chae[4]

[1]La Canada High School, La Canada, California, USA
[2]Village Christian School, Sun Valley, California, USA
[3]South Torrance High School, Torrance, California, USA
[4]Le Lycee Francais de Los Angeles, Los Angeles, California, USA

Advisor: Chris Cha, iANT Education, chrisiantedu@gmail.com

Abstract

Dietary supplements can carry trace metal contamination, yet this hazard is rarely screened. Copper, zinc, and iron enter multivitamin, herbal, and algal products through raw material residues or deliberate fortification. Inductively coupled plasma mass spectrometry (ICP-MS) reports metal content but not biological toxicity, which depends on bioavailability and matrix chemistry. We built a low-cost dual-species bacterial biosensor that reads out metal toxicity as a growth-inhibition signature. *Escherichia coli* C600 (Gram-negative) and *Bacillus megaterium* (Gram-positive) were incubated with three reference metals ($CuSO_4 \cdot 5H_2O$, $ZnSO_4 \cdot 7H_2O$, $FeSO_4 \cdot 6H_2O$) at 0, 1, 10, and 50 ppm, and with three commercial supplements (Ashwagandha, Multivitamin, Spirulina) as 10% v/v aqueous extracts. Growth was tracked over 6 hours by OD_{600} in liquid cuvettes at 90-minute intervals and by endpoint colony counts on metal-loaded LB agar. One-way ANOVA with Tukey HSD and two-way ANOVA tested concentration and species × concentration effects. All six species × metal ANOVAs were significant ($p < 0.001$), and *B. megaterium* was 4–5× more sensitive than *E. coli* to Cu and Zn. Species × concentration interactions were also significant by two-way ANOVA ($p < 0.01$). Multivitamin extract inhibited growth to a level comparable with ~10 ppm Cu exposure; Spirulina suppressed apparent OD without a matching drop in colony count, which identified that signal as pigment interference rather than toxicity. The Gram-type-specific inhibition fingerprints support the dual-species, dual-readout platform as a rapid biological screen for trace metal contamination in dietary supplements.

Keywords: *trace metals; dietary supplements; biosensor; Escherichia coli; Bacillus megaterium; growth inhibition; gut microbiome; ICP-MS alternative; ANOVA*

1. Introduction

Trace metals shape microbial ecosystems in the human body. Zinc, copper, and iron in dietary supplements support bone development, immune regulation, and many other physiological functions, but the same metals can shift the composition of the gut microbiome when they are in short supply or in excess. Because many gut bacteria depend on tightly regulated intracellular metal pools, even small imbalances can disturb microbial homeostasis. At balanced levels, trace metals sustain the growth of beneficial genera such as *Lactobacillus* and *Bifidobacterium* (Huynh et al., 2022). At elevated levels they suppress these protective species and favor more resistant, sometimes pathogenic, strains (Bushman & Skaar, 2025).

Excess zinc lowers microbial diversity and enriches zinc-tolerant, occasionally pathogenic, bacteria. Elevated copper acts as an antimicrobial by generating oxidative stress and damaging bacterial membranes, cutting into beneficial populations. Irregular iron delivery favors pathogens over commensals. This kind of metal-driven dysbiosis has been tied to reduced microbial diversity, weakened immune regulation, and impaired colonization resistance (Bushman & Skaar, 2025), and is associated with constipation, diarrhea, and fatigue in supplement users.

The risks are not hypothetical. Case reports document hepatotoxicity, hematologic disturbance, and gastrointestinal symptoms after excessive vitamin and mineral intake, and toxic ingestions of iron- and copper-containing supplements continue to appear in the literature (Wooltorton, 2003). Regulatory oversight of trace metal content in supplements remains lighter than for pharmaceuticals or food. ICP-MS and graphite furnace atomic absorption spectrometry can quantify metals at very low levels (El Hosry et al., 2023), and newer platforms including ion-current-rectifying quartz nanopipettes have been

proposed for trace metal detection in organic products (Farrell et al., 2024). These chemical measurements report concentration, not bioavailability or biological toxicity in a gut-like environment.

Bacterial responses to metals are shaped by cell wall architecture. Gram-positive bacteria have a thick peptidoglycan wall and no outer lipid membrane; they are monoderms. This dense wall traps the iodine-crystal violet complex during Gram staining, so the cells appear purple. Gram-negative bacteria have a thin peptidoglycan layer beneath an outer membrane rich in lipopolysaccharides — diderms. Alcohol strips the outer membrane, the primary stain washes out, and the cells take up the pink safranin counterstain. These structural differences matter for more than staining: they govern how bacteria interact with their environment (Silhavy et al., 2010). The Gram-negative outer membrane is a selective barrier that raises tolerance to antibiotics, detergents, and metal stress. Gram-positive walls lack this outer membrane but contain teichoic and lipoteichoic acids that contribute to structural stability and, through their negative charges, to metal binding. Cell wall architecture therefore drives metal uptake, tolerance, and toxicity.

Bacteria in a closed system grow through predictable phases. During the lag phase, cells adjust to the medium and synthesize enzymes without dividing. In the exponential (log) phase, cells divide at their maximal rate and the population doubles at fixed intervals as nutrients are consumed. As nutrients run out and waste accumulates, growth slows through a deceleration phase into stationary phase, where division rate equals death rate. In the death phase, viability declines. Two parameters quantify this process: the specific growth rate (μ), which describes exponential-phase population expansion, and the yield coefficient (Y), which relates new biomass to substrate consumed. Deviations in these parameters flag the effect of external stressors such as trace metals.

We used *Escherichia coli* C600 as a Gram-negative model and *Bacillus megaterium* as a Gram-positive model to test dose-dependent effects of copper, zinc, and iron on bacterial growth. *E. coli* suits this role because it grows fast, its physiology is well characterized, and it is a gut commensal. By exposing both organisms to a defined concentration series drawn from certified metal standards and from commercially available dietary supplements, and by reading OD_{600} as a proxy for growth, the assay produces a quantitative record of how supplement-derived metals could affect gut microbial populations.

2. Materials and Methods

2.1 Bacterial Strains and Culture Conditions

Two bacterial strains were used: *Escherichia coli* C600 (Gram-negative) and *Bacillus megaterium* (Gram-positive). Group labels used throughout follow Gram stain: (+) for Gram-positive (*B. megaterium*) and (−) for Gram-negative (*E. coli*). Slant cultures were held at 4°C. Working inocula were prepared by scraping a loopful of cells from each slant into 5 mL of sterile LB and vortexing for 30 s. Each suspension was measured at OD_{600} and diluted to $OD_{600} \approx 0.5$ using $C_1V_1 = C_2V_2$. All cultures were incubated at 37°C in static conditions.

2.2 Preparation of Metal Stock Solutions

Stock solutions of copper, zinc, and iron were prepared at 1000 ppm by dissolving $CuSO_4 \cdot 5H_2O$ (0.3928 g per 100 mL), $ZnSO_4 \cdot 7H_2O$ (0.4398 g per 100 mL), and $FeSO_4 \cdot 7H_2O$ (0.4655 g per 100 mL) in deionized water. One drop of dilute HCl was added to the $FeSO_4$ stock to limit Fe^{2+} oxidation to Fe^{3+}. Each 1000 ppm stock was diluted 10-fold to a 100 ppm working stock. Final exposure concentrations of 0, 1, 10, and 50 ppm were prepared by volumetric dilution into sterile LB broth to 1.35 mL per cuvette (Table 1).

Table 1. Metal solution dilution scheme for cuvette preparation.

Final concentration (ppm)	100 ppm stock (μL)	Sterile LB (μL)	Total (μL)
0 (control)	0	1350	1350
1	13.5	1336.5	1350
10	135	1215	1350
50	675	675	1350

2.3 Preparation of Dietary Supplement Extracts

Water-soluble fractions were prepared from three commercial supplements: Ashwagandha, Multivitamin, and Spirulina. For each, 1.0 g of finely ground powder was suspended in 10 mL of deionized water, vortexed for 1 min, and left to settle for 10 min. The supernatant was filtered through a coffee filter to remove particulate material. Each extract was added to bacterial cultures at 10% v/v. Coffee filtration does not sterilize the extract, but no microbial growth appeared in supplement-only no-cell controls except for one Multivitamin replicate (Section 2.5).

2.4 Growth Assay Setup

Each cuvette received 1.35 mL of treatment broth (metal solution, supplement extract, or plain LB) followed by 0.15 mL of the appropriate working inoculum, for a total volume of 1.5 mL and a starting OD_{600} of about 0.05 after 10-fold dilution of the OD 0.5 inoculum. No-cell control cuvettes received 1.35 mL of treatment broth only. Cuvettes were sealed with Parafilm and incubated statically at 37°C. OD_{600} was read every 90 minutes for 6 hours (T = 0, 1.5, 3.0, 4.5, and 6.0 h) against sterile LB as the instrument blank. Each condition was run in biological triplicate.

2.5 Data Analysis and Quality Control

Raw OD_{600} values were corrected for background absorbance by subtracting the grand mean of the matched no-cell control across all timepoints and replicates. No-cell controls showed no temporal drift (SD ≤ 0.007 OD units), which justified the grand-mean approach. The LB blank (grand mean = 0.040) was used for Cu 0–10 ppm and Zn 0–10 ppm, because $CuSO_4$ and $ZnSO_4$ contribute negligible OD_{600}. Matched metal-only controls were used for Cu 50 ppm (0.043) and Zn 50 ppm (0.046). For iron, mild Fe^{2+} oxidation produced a precipitate that raised the 50 ppm no-cell blank to 0.072; the Fe 50 ppm no-cell control was therefore used at that concentration, and the LB blank was used for Fe 0–10 ppm. Supplement-only no-cell controls were used for Ashwagandha (0.062) and Multivitamin (0.069). Negative corrected OD values were floored to zero for plotting. Spirulina OD_{600} data were excluded from all growth analyses because chlorophyll and phycocyanin produced a background of about 0.24, which swamped the bacterial signal.

The following individual data points were excluded on the basis of documented procedural anomalies: Cu 10 ppm *E. coli* replicate 2 (suspected pipetting error; growth profile matched the 1 ppm condition); Zn 50 ppm *E. coli* replicate 3 (suspected contamination; OD exceeded 1.4 by T = 6h with visible turbidity change); Fe 10 ppm *B. megaterium* replicate 1 at T = 3h (bubble artifact; OD = 0.851 versus 0.127–0.156 in co-replicates); and Multivitamin no-cell control replicate 2 (OD rose from 0.082 to 0.258 in the absence of cells, consistent with contamination or mislabeling). Cu 1 ppm *B. megaterium* replicate 3 was missing the T = 4.5 h reading due to instrument availability; the mean at that timepoint was computed from the remaining two replicates.

Specific growth rates (μ, h^{-1}) were computed with the two-point formula $\mu = (\ln OD_2 - \ln OD_1) / (t_2 - t_1)$, applied to the steepest consecutive 90-minute interval in the log-linear phase for each condition. Growth-rate calculations were restricted to timepoints with corrected OD > 0.02, roughly three times the SD of the most variable no-cell control (Fe blank SD = 0.007). When no timepoint pair met this criterion, μ was reported as not calculable (NC), which indicates effective growth inhibition. Exponential phase windows were selected independently for *E. coli* and *B. megaterium* to reflect their different kinetics. The 6-hour window was too short for control and low-concentration cultures to reach stationary phase, so OD at T = 6h is reported here as a terminal growth index, not maximum OD. To capture cumulative growth across the time course, the area under the growth curve (AUC) was computed for each replicate by the trapezoidal rule across all five timepoints and used as the primary response variable. Results are mean ± SD across biological triplicates (or duplicates where one replicate was excluded). IC_{50} was not fit numerically because the concentration series (0, 1, 10, 50 ppm) is too coarse to bracket the 50% point; the interval within which 50% inhibition occurs is reported instead. The 0 ppm control OD at T = 6h varied modestly across metal series (*E. coli*: 0.595–0.661; *B. megaterium*: 0.351–0.372), consistent with small differences in inoculum handling and incubator position. Inhibited conditions were therefore normalized to their own metal-series 0 ppm control rather than a pooled mean.

Statistical analyses were run in three groups. Metal-concentration effects on AUC within each metal × species combination were tested by one-way ANOVA with Tukey post-hoc comparisons and Bonferroni correction for six comparisons per group. Levene's test confirmed homogeneity of variance (all $p > 0.25$), which supports standard ANOVA. Species differences at each metal concentration were tested by independent-samples Welch's t-tests with Bonferroni correction for 12 comparisons per metal (adjusted $\alpha = 0.0042$). Supplement effects on AUC relative to the LB control (Cu series 0 ppm) were tested by independent-samples Welch's t-tests with Bonferroni correction for four comparisons (adjusted $\alpha = 0.0125$). Conditions with n = 2 after replicate exclusion were reported descriptively rather than entered into ANOVA. Significance is denoted * $p < 0.05$, ** $p < 0.01$, *** $p < 0.001$, and ns (not significant).

3. Results

3.1 No-Cell Control Validation

No-cell controls confirmed that sterile LB and the Cu and Zn metal solutions did not contribute meaningful OD_{600}. The LB blank was stable across timepoints and replicates (grand mean = 0.040, SD = 0.003), as were Cu and Zn no-cell controls (Cu: 0.043 ± 0.003; Zn: 0.046 ± 0.005). The Fe 50 ppm no-cell control was elevated (grand mean = 0.072 ± 0.007), consistent with light scattering from iron hydroxide precipitate that persisted despite the dilute HCl added during stock preparation. Ashwagandha extract gave a stable background of 0.062 ± 0.004, and Multivitamin extract (replicates 1 and 3 only) gave 0.069 ± 0.005. Spirulina extract produced a background OD_{600} of about 0.24 across all replicates, driven by the strong absorption of photosynthetic pigments. This level of optical interference ruled out OD_{600} as a growth proxy for Spirulina, and those data were dropped from further analysis.

3.2 Area Under the Growth Curve

AUC values (OD_{600}·h) computed by the trapezoidal rule across all five timepoints are given in Table 2 and served as the primary response variable. In the absence of metal, *E. coli* AUC ranged from 1.54 ± 0.10 (Cu series) to 1.62 ± 0.09 (Fe series), and *B. megaterium* AUC ranged from 0.84 ± 0.02 (Zn series) to 0.86 ± 0.11 (Cu series). Baseline AUC was consistently lower for *B. megaterium*, reflecting its slower intrinsic growth rate. AUC decreased monotonically with concentration for both species, except for *E. coli* under iron, where AUC at 1 ppm (1.62 ± 0.08) matched the 0 ppm control (1.61 ± 0.09) and AUC at 10 ppm (1.32 ± 0.05) stayed well above the inhibitory range (Figure 1).

Table 2. Area under the growth curve (AUC, OD_{600}·h) for all conditions, calculated by the trapezoidal rule across T = 0–6h after background subtraction. Values are mean ± SD across biological replicates.

Metal / Supp	Species	Conc.	AUC mean	AUC SD	n
Cu	E. coli (−)	0 ppm	1.543	0.097	3
	E. coli (−)	1 ppm	1.307	0.028	3
	E. coli (−)	10 ppm	0.540	0.020	2*
	E. coli (−)	50 ppm	0.119	0.017	3
	B. megaterium (+)	0 ppm	0.856	0.111	3
	B. megaterium (+)	1 ppm	0.332	0.204	3
	B. megaterium (+)	10 ppm	0.144	0.069	3
	B. megaterium (+)	50 ppm	0.049	0.037	3
Zn	E. coli (−)	0 ppm	1.616	0.101	3
	E. coli (−)	1 ppm	1.467	0.114	3
	E. coli (−)	10 ppm	0.550	0.084	3
	E. coli (−)	50 ppm	0.154	0.001	2†
	B. megaterium (+)	0 ppm	0.843	0.017	3
	B. megaterium (+)	1 ppm	0.418	0.044	3
	B. megaterium (+)	10 ppm	0.074	0.015	3
	B. megaterium (+)	50 ppm	0.059	0.042	3
Fe	E. coli (−)	0 ppm	1.607	0.089	3

Metal / Supp	Species	Conc.	AUC mean	AUC SD	n
	E. coli (−)	1 ppm	1.617	0.078	3
	E. coli (−)	10 ppm	1.323	0.051	3
	E. coli (−)	50 ppm	0.208	0.020	3
	B. megaterium (+)	0 ppm	0.832	0.039	3
	B. megaterium (+)	1 ppm	0.776	0.026	3
	B. megaterium (+)	10 ppm	0.473	0.181	3‡
	B. megaterium (+)	50 ppm	0.054	0.029	3
Ashwagandha	E. coli (−)	10% v/v	0.604	0.010	3
	B. megaterium (+)	10% v/v	0.270	0.132	3
Multivitamin	E. coli (−)	10% v/v	0.429	0.103	3
	B. megaterium (+)	10% v/v	0.019	0.009	3
Spirulina	Both	10% v/v	Excluded	—	—

*n = 2 (Cu 10 ppm E. coli, replicate excluded — pipetting error). † n = 2 (Zn 50 ppm E. coli, replicate excluded — contamination). ‡ Fe 10 ppm B. megaterium: n = 3 but T = 3h reading excluded from one replicate (bubble artifact); elevated SD reflects residual inter-replicate variability.

Lower AUC indicates stronger growth suppression. Across all metals (Cu, Zn, Fe) and both supplement extracts, AUC dropped sharply with concentration for both *E. coli* and *B. megaterium*. The Multivitamin extract and the 50 ppm Cu and Zn conditions drove growth to near zero.

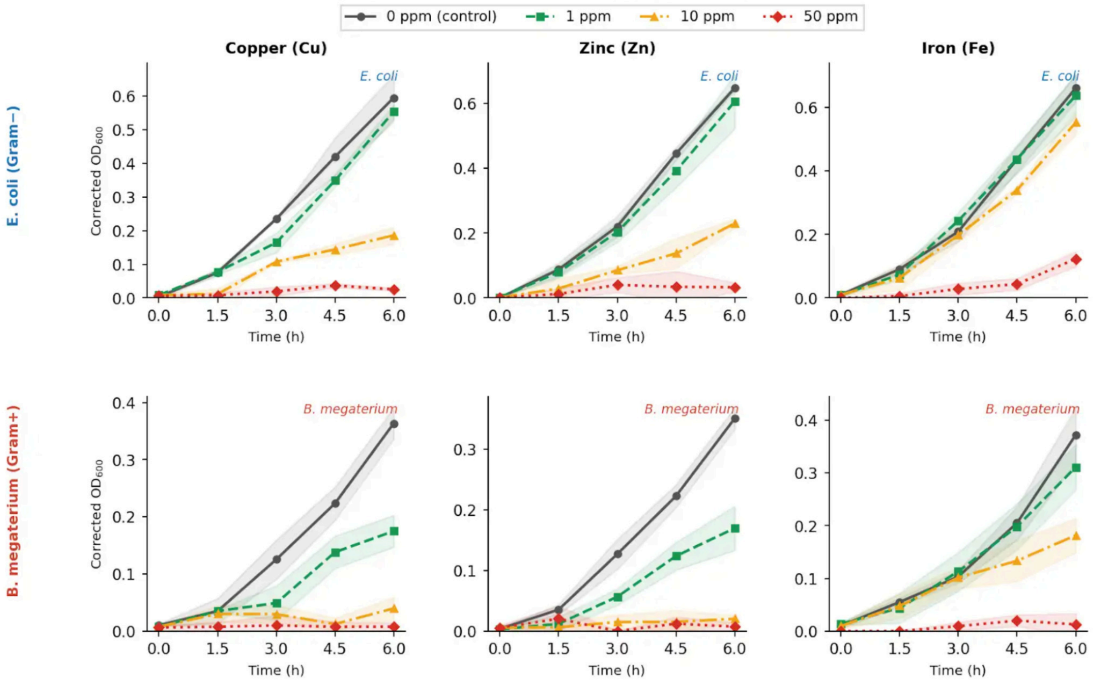

Figure 1. Growth curves of *E. coli* C600 and *B. megaterium* under copper, zinc, and iron at 0, 1, 10, and 50 ppm. OD_{600} was read every 90 minutes for 6 hours. Each curve is the mean of biological triplicates after background subtraction; shaded bands are ± 1 SD.

Gram (−):

All three metals inhibited *E. coli* in a dose-dependent way, but the toxicity threshold differed by metal. Copper and zinc behaved similarly: growth was cut sharply at 10 ppm and nearly abolished at 50 ppm, where AUC fell to about 0.12 (Cu) and 0.15 (Zn) — roughly 90% below control. Inhibition was most visible in the 3–6 h exponential phase. Iron was different. At 1 ppm, growth matched the untreated control, consistent with iron acting as an essential micronutrient at trace levels. Meaningful inhibition only appeared at 10 ppm and above. Iron's transition from nutrient to toxin sits at a higher concentration than copper or zinc.

3.3 Effect of Copper on Bacterial Growth

Copper inhibited growth in both species in a dose-dependent way, with *B. megaterium* more sensitive than *E. coli* at matched concentrations (Figure 2). One-way ANOVA showed a significant effect of Cu concentration on AUC for both *E. coli* ($F = 413.7$, $p < 0.001$) and *B. megaterium* ($F = 25.8$, $p < 0.001$). Without metal, *E. coli* reached corrected OD_{600} 0.595 ± 0.069 at T = 6h with $\mu = 0.762 \pm 0.080$ h^{-1} and AUC = 1.543 ± 0.097; *B. megaterium* reached OD 0.363 ± 0.027 with $\mu = 0.545 \pm 0.239$ h^{-1} and AUC = 0.856 ± 0.111. At 1 ppm Cu, *E. coli* growth was slightly reduced (AUC = 1.307 ± 0.028; p_adj = 0.260 vs control), while *B. megaterium* dropped more sharply (AUC = 0.332 ± 0.204; p_adj = 0.170) with the exponential phase pushed back to the 3.0–4.5 h interval. At 10 ppm, *E. coli* AUC was reduced against both control (p_adj = 0.012) and 1 ppm (p_adj = 0.0004), and *B. megaterium* growth was effectively abolished (μ = NC; AUC = 0.144 ± 0.069; p_adj = 0.010 vs control). At 50 ppm, both species were near-completely inhibited (μ = NC; *E. coli* AUC = 0.119 ± 0.017; *B. megaterium* AUC = 0.049 ± 0.037; p_adj ≤ 0.019 vs their respective controls). Pairwise comparisons among the 1, 10, and 50 ppm *B. megaterium* groups were all non-significant (p_adj ≥ 0.746), which indicates that Cu inhibition saturates at 1 ppm. IC_{50} fell between 1 and 10 ppm for *E. coli* and between 0 and 1 ppm for *B. megaterium*.

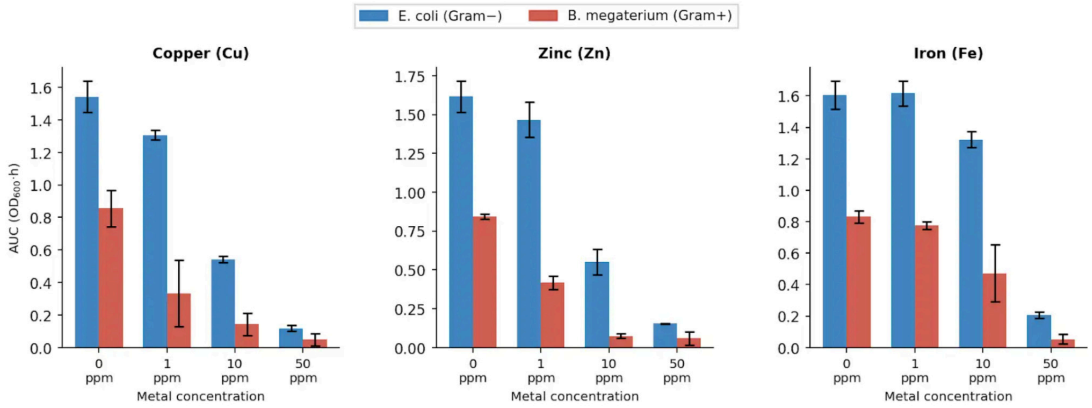

Figure 2. Copper ($CuSO_4 \cdot 5H_2O$) effect on bacterial growth. Left: *E. coli* C600 at 0, 1, 10, and 50 ppm Cu. Right: *B. megaterium* under the same conditions. OD_{600} was read every 90 minutes across biological triplicates; shaded bands are ± 1 SD. Significance markers refer to Tukey HSD post-hoc comparisons versus the 0 ppm control (* p_adj < 0.05, ** p_adj < 0.01, *** p_adj < 0.001).

3.4 Effect of Zinc on Bacterial Growth

Zinc produced the sharpest species split of any metal (Figure 3). One-way ANOVA gave a significant effect of Zn on AUC for both *E. coli* ($F = 148.6$, $p < 0.001$) and *B. megaterium* ($F = 383.5$, $p < 0.001$). *E. coli* tolerated low Zn well: at 1 ppm, AUC (1.467 ± 0.114) did not differ from control (1.616 ± 0.101; p_adj = 0.991), and μ was essentially unchanged (0.633 ± 0.055 vs 0.628 ± 0.109 h^{-1}). Even at 10 ppm, a calculable growth rate was retained ($\mu = 0.605 \pm 0.201$ h^{-1}), although AUC was reduced against both 0 ppm (p_adj = 0.001) and 1 ppm (p_adj = 0.003). *B. megaterium* was already suppressed at 1 ppm (AUC = 0.418 ± 0.044; p_adj = 0.007 vs control) and completely inhibited at 10 and 50 ppm (μ = NC; AUC = 0.074 ± 0.015 and 0.059 ±

0.042; both p_adj < 0.002 vs control). The pairwise 10 vs 50 ppm comparison for *B. megaterium* was non-significant (p_adj = 1.000), consistent with saturating inhibition. IC_{50} fell between 1 and 10 ppm for *E. coli* and between 0 and 1 ppm for *B. megaterium*. The *E. coli* Zn 50 ppm mean rests on two replicates and is reported descriptively.

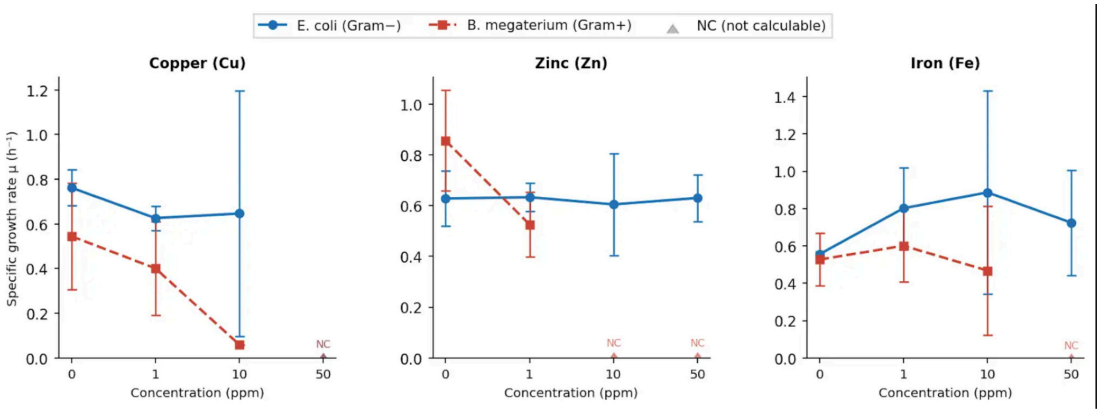

Figure 3. Zinc ($ZnSO_4 \cdot 7H_2O$) effect on bacterial growth. Left: *E. coli* C600; right: *B. megaterium*. Same experimental scheme and annotation conventions as Figure 2.

3.5 Effect of Iron on Bacterial Growth

Iron gave a different dose-response than copper or zinc, especially for *E. coli* (Figure 4). One-way ANOVA confirmed a significant effect of Fe on AUC for both *E. coli* ($F = 315.2$, $p < 0.001$) and *B. megaterium* ($F = 42.8$, $p < 0.001$). Instead of monotonic inhibition, *E. coli* grew as well or better at 1 and 10 ppm Fe than at 0. AUC at 1 ppm (1.617 ± 0.078) matched the 0 ppm control (1.607 ± 0.089; p_adj = 1.000), and AUC at 10 ppm (1.323 ± 0.051) did not differ from control (p_adj = 0.090) or 1 ppm (p_adj = 0.051). Growth rates at 1 ppm ($\mu = 0.802 \pm 0.219$ h^{-1}) and 10 ppm ($\mu = 0.887 \pm 0.546$ h^{-1}) exceeded the control ($\mu = 0.556 \pm 0.015$ h^{-1}), suggesting the LB medium was mildly iron-limited and that supplemental iron at these levels was growth-promoting. None of these curves reached stationary phase within 6 h. Only at 50 ppm Fe was AUC reduced against both control (p_adj = 0.005) and 1 ppm (p_adj = 0.003), with growth delayed and μ calculable only from the late interval (T = 4.5–6 h; $\mu = 0.724 \pm 0.281$ h^{-1}). *B. megaterium* showed the more usual monotonic inhibition: AUC at 1 ppm (0.776 ± 0.026) did not differ from control (0.832 ± 0.039; p_adj = 0.716), AUC at 10 ppm (0.473 ± 0.181) was likewise non-significant (p_adj = 0.415), and only 50 ppm was significantly different from both control and 1 ppm (both p_adj < 0.0001; AUC = 0.054 ± 0.029; μ = NC). The large SD at 10 ppm reflects the single replicate affected by a bubble artifact. IC_{50} fell between 10 and 50 ppm for *E. coli* and between 1 and 10 ppm for *B. megaterium*.

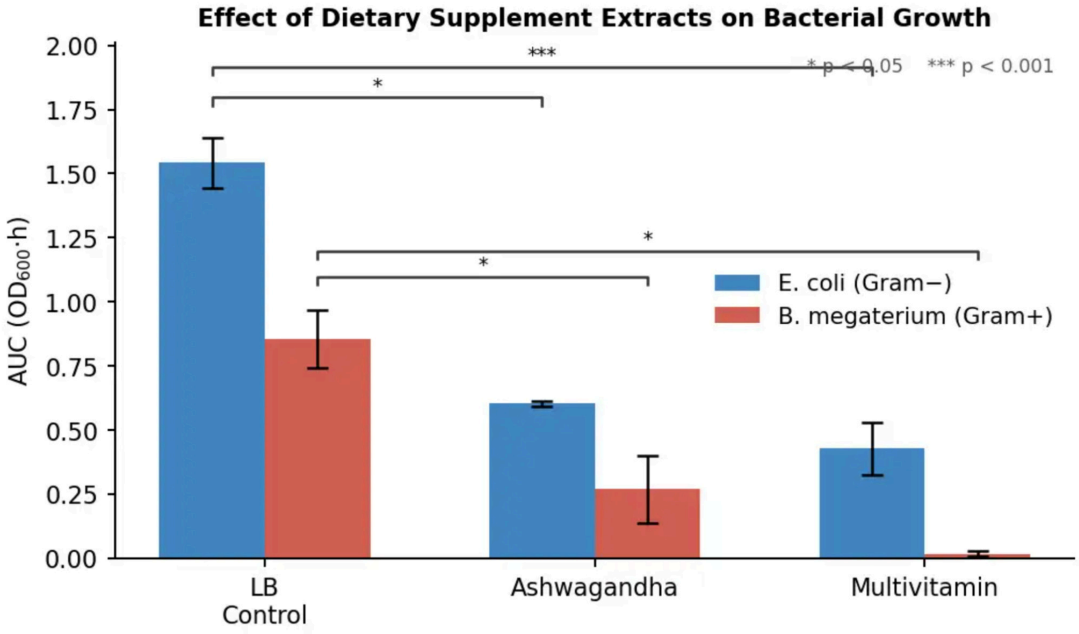

Figure 4. Iron ($FeSO_4 \cdot 6H_2O$) effect on bacterial growth. Left: *E. coli* C600 shows a biphasic response (mild stimulation at 1 and 10 ppm, inhibition at 50 ppm); right: *B. megaterium* shows monotonic inhibition. Annotation conventions as in Figure 2.

3.6 Effect of Dietary Supplement Extracts on Bacterial Growth

Ashwagandha and Multivitamin extracts both reduced bacterial growth relative to the LB control. In both extract conditions, the exponential phase did not start until the T = 4.5–6 h interval, compared with T = 1.5–3 h in most metal controls, which points to an extended lag phase in the presence of the supplement matrix.

Ashwagandha extract reduced AUC in both species (*E. coli*: 0.604 ± 0.010 vs control 1.543 ± 0.097, p_adj = 0.013; *B. megaterium*: 0.270 ± 0.132 vs control 0.856 ± 0.111, p_adj = 0.018). Both species retained measurable growth above corrected background (μ = 0.237 ± 0.175 and 0.320 ± 0.107 h^{-1} for *E. coli* and *B. megaterium*), so inhibition was partial. The high replicate spread in *B. megaterium* Ashwagandha cultures (AUC SD = 0.132) reflects divergent growth trajectories, possibly from variable bioavailability of the extract's inhibitory compounds.

Multivitamin extract split the two species. *E. coli* AUC was reduced against control (0.429 ± 0.103 vs 1.543 ± 0.097; p_adj < 0.001) but growth remained detectable (μ = 0.678 ± 0.170 h^{-1}). *B. megaterium* corrected OD never rose above the 0.02 detection threshold at any timepoint or replicate (μ = NC; AUC = 0.019 ± 0.009; p_adj = 0.023 vs control) — effectively complete inhibition. The Gram-positive-selective effect matches what Cu and Zn produced and points to metal or bioactive components in the Multivitamin that hit *B. megaterium* harder. Spirulina OD_{600} data were excluded as described in Section 2.5 (Figure 5).

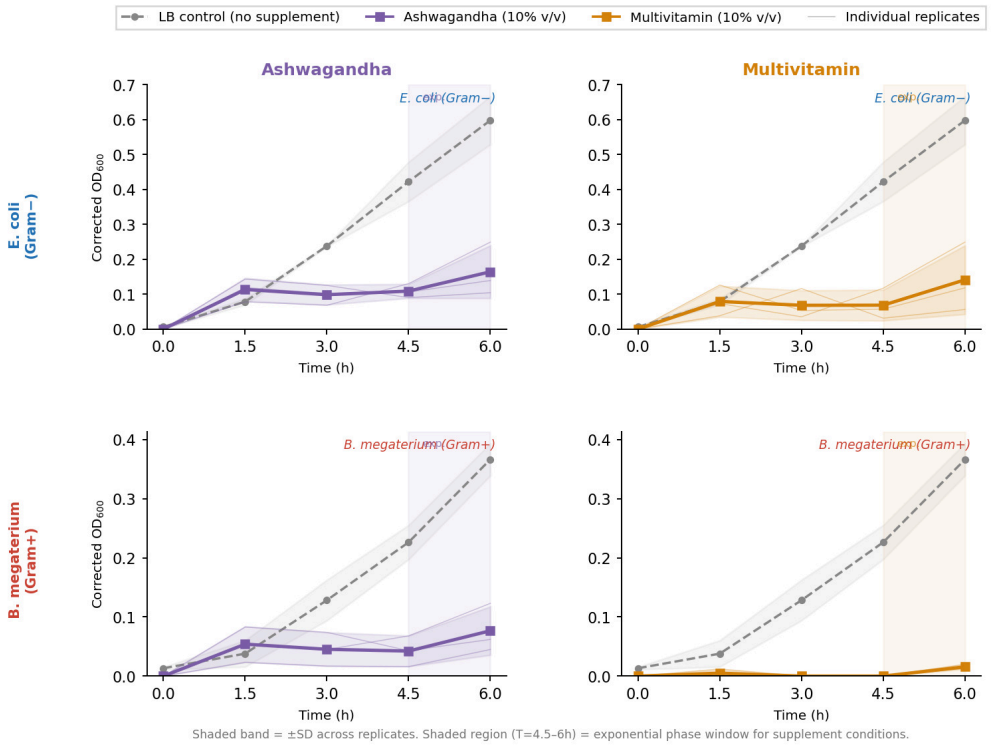

Figure 5. Dietary supplement extract effects on bacterial growth. *E. coli* C600 and *B. megaterium* exposed to Ashwagandha and Multivitamin extracts at 10% v/v against the LB control. Spirulina was excluded because of pigment interference (Section 3.1). Shaded bands are ± 1 SD across biological triplicates.

Gram (−):

Both Ashwagandha and Multivitamin extracts inhibited *E. coli* growth against the LB control without abolishing it. With Ashwagandha at 10% v/v, growth was suppressed throughout, and the gap between the treated and control curves widened most between 4.5 and 6 h, where the treated culture plateaued below the control trajectory. AUC = 0.604 reflects moderate but steady inhibition. Multivitamin produced a similar shape with greater replicate spread (wider shaded band). Its AUC of 0.429 sits slightly below Ashwagandha, but the difference is small relative to the spread. In both cases, *E. coli* kept growing rather than being arrested — partial inhibition, not complete.

3.7 Species Comparison and Summary of Growth Parameters

Across all three metals, *E. coli* AUC exceeded *B. megaterium* AUC at every concentration tested, with the gap ranging from 0.069 (Cu 50 ppm) to 1.115 (Fe 10 ppm). Species differences were statistically significant (Bonferroni-corrected Welch's t-test) at Cu 0 ppm (p_adj = 0.017), Zn 1 ppm (p_adj = 0.017), Fe 0 ppm (p_adj = 0.016), Fe 1 ppm (p_adj = 0.015), and Fe 50 ppm (p_adj = 0.031). Many comparisons failed to clear significance despite large mean differences, reflecting the low statistical power of n = 3 combined with Bonferroni correction across 12 comparisons. The directional pattern was nevertheless consistent: *B. megaterium* was more sensitive to metal exposure than *E. coli* under every condition tested. Specific growth rates and OD at T = 6h are summarized in Table 3.

Table 3. Specific growth rates (μ) and OD_{600} at T = 6h for all conditions. OD at T = 6h is a terminal growth index; stationary phase was not reached in control and low-concentration conditions within the 6-hour window. Values are mean ± SD across biological replicates. NC = not calculable (corrected OD did not exceed the 0.02 detection threshold).

Metal / Supp	Species	Conc (ppm)	μ (h^{-1})	OD at T=6h	Interval	n
Cu	E. coli (−)	0	0.762 ± 0.080	0.595 ± 0.069	1.5–3h	3

Metal / Supp	Species	Conc (ppm)	μ (h^{-1})	OD at T=6h	Interval	n
	E. coli (−)	1	0.626 ± 0.055	0.554 ± 0.020	1.5–3h	3
	E. coli (−)	10	0.647 ± 0.551*	0.186 ± 0.026	3–4.5h	2*
	E. coli (−)	50	NC	0.025 ± 0.004	—	3
	B. megaterium (+)	0	0.545 ± 0.239	0.363 ± 0.027	1.5–3h	3
	B. megaterium (+)	1	0.401 ± 0.209	0.175 ± 0.028	3–4.5h	3
	B. megaterium (+)	10	NC	0.040 ± 0.020	—	3
	B. megaterium (+)	50	NC	0.008 ± 0.007	—	3
Zn	E. coli (−)	0	0.628 ± 0.109	0.648 ± 0.008	1.5–3h	3
	E. coli (−)	1	0.633 ± 0.055	0.606 ± 0.083	1.5–3h	3
	E. coli (−)	10	0.605 ± 0.201	0.230 ± 0.014	1.5–3h	3
	E. coli (−)	50	0.630 ± 0.092†	0.033 ± 0.015	NC†	2†
	B. megaterium (+)	0	0.856 ± 0.198	0.351 ± 0.018	1.5–3h	3
	B. megaterium (+)	1	0.526 ± 0.128	0.170 ± 0.036	3–4.5h	3
	B. megaterium (+)	10	NC	0.020 ± 0.006	—	3
	B. megaterium (+)	50	NC	0.007 ± 0.006	—	3
Fe	E. coli (−)	0	0.556 ± 0.015	0.661 ± 0.042	1.5–3h	3
	E. coli (−)	1	0.802 ± 0.219	0.637 ± 0.067	1.5–3h	3
	E. coli (−)	10	0.887 ± 0.546	0.553 ± 0.036	1.5–3h	3
	E. coli (−)	50	0.724 ± 0.281	0.123 ± 0.024	4.5–6h	3
	B. megaterium (+)	0	0.527 ± 0.141	0.372 ± 0.052	3–4.5h	3
	B. megaterium (+)	1	0.601 ± 0.194	0.311 ± 0.043	1.5–3h	3
	B. megaterium (+)	10	0.468 ± 0.344	0.182 ± 0.032	1.5–3h	3
	B. megaterium (+)	50	NC	0.013 ± 0.021	—	3
Ashwagandha	E. coli (−)	10% v/v	0.237 ± 0.175	0.164 ± 0.076	4.5–6h	3
	B. megaterium (+)	10% v/v	0.320 ± 0.107	0.077 ± 0.041	4.5–6h	3
Multivitamin	E. coli (−)	10% v/v	0.678 ± 0.170	0.141 ± 0.099	4.5–6h	3
	B. megaterium (+)	10% v/v	NC	0.016 ± 0.004	—	3
Spirulina	Both	10% v/v	Excluded	Excluded	—	—

*n = 2 after exclusion of replicate with suspected pipetting error; μ SD unreliable. † n = 2 after exclusion of contaminated replicate; μ derived from mean curve and should be read with caution given very low corrected OD.

3.8 Colony Count Validation

Bacterial viability was assessed in parallel with spot plates on LB agar, with colonies counted after overnight incubation at 37°C. Colony counts are single-replicate observations (n = 1 per condition) and are treated here as corroborating evidence for the liquid culture OD results rather than as an independent statistical dataset. Percent inhibition was computed against the matched 0 ppm control for metal conditions and against the species growth control for supplement conditions. Three data points carry quality flags: *E. coli* Cu 10 ppm (unidentified white colonies alongside typical *E. coli* colonies; only morphologically typical colonies were counted); *B. megaterium* Zn 1 ppm (spreader adhesion smeared the plate; count of ≈83 is approximate); and *E. coli* Fe 10 ppm (plate broken during transfer; no count recorded). No-cell control plates (LB blank, Cu 50 ppm, Zn 50 ppm, and Fe 50 ppm without bacteria) produced zero colonies, confirming that the metal solutions and sterile LB were uncontaminated.

Colony counts matched OD-based trends across the metal conditions. For copper, both species showed dose-dependent CFU reductions: *E. coli* inhibition ran from 11.6% at 1 ppm to 67.1% at 10 ppm and 95.4% at 50 ppm, while *B. megaterium* hit 38.6% at 1 ppm and near-complete suppression at 10 ppm (91.5%) and 50 ppm (94.7%), matching the earlier saturation seen in the OD data. For zinc, *E. coli* showed 24.8% inhibition at 1 ppm, 52.3% at 10 ppm, and 93.9% at 50 ppm. *B. megaterium* was more sensitive: 59.7% inhibition at 1 ppm (approximate count) and ≥94.7% at 10 and 50 ppm, matching effective growth abolition at those concentrations. For iron, both species showed mild inhibition at 1 ppm (*E. coli*: 7.0%; *B. megaterium*: 15.0%), rising with concentration. The *E. coli* Fe 10 ppm plate was unavailable, so the stimulatory iron effect seen by OD was not validated on plates. At 50 ppm Fe, *E. coli* colony count inhibition (57.0%) was lower than the OD-AUC estimate implied (87%), consistent with Fe precipitate scattering over-correcting the OD baseline at this concentration — the plate count is the more reliable readout there.

For the supplement conditions, colony counts revealed a large split with the OD results for Ashwagandha-treated *E. coli*. Plate counts showed only 1.9% inhibition (203 vs growth control 207) — essentially no drop in viability — while OD AUC indicated a 61% reduction in cumulative growth relative to the LB control. Ashwagandha extract acts bacteriostatically against *E. coli*: cells stay viable and can form colonies but stop dividing at the normal rate during liquid culture. The extended lag phase in the OD growth curves fits this reading. *B. megaterium*, by contrast, showed 76.6% colony count inhibition under Ashwagandha (51 vs 218) — genuine growth suppression, not just a growth-rate effect. Multivitamin extract produced 55.6% colony count inhibition in *E. coli* and 93.1% in *B. megaterium*, in line with the OD reading of near-complete *B. megaterium* suppression.

Colony counts also provided the only quantitative readout for Spirulina, whose OD_{600} was ruled out by pigment interference. *E. coli* treated with Spirulina at 10% v/v yielded 225 colonies vs a growth control of 207 (−8.7%; no inhibition, marginal apparent stimulation within noise). *B. megaterium* showed 28.0% inhibition (157 vs 218). Spirulina extract does not inhibit *E. coli* viability at 10% v/v but produces moderate inhibition of *B. megaterium*, extending the Gram-positive-selective inhibition pattern to a third supplement. All colony count data and percent inhibition values appear in Table 4.

Table 4. Colony counts and percent inhibition against matched controls for all conditions. Colony counts are single-replicate spot plate observations (n = 1). Percent inhibition = (1 − count/control) × 100; negative values indicate apparent stimulation.

Species	Treatment	Conc.	Count	Control	% inhibition
E. coli (−)	Cu	0 ppm	216	—	reference
	Cu	1 ppm	191	216	11.6%
	Cu	10 ppm	71	216	67.1%
	Cu	50 ppm	10	216	95.4%
	Zn	0 ppm	262	—	reference
	Zn	1 ppm	197	262	24.8%
	Zn	10 ppm	125	262	52.3%
	Zn	50 ppm	16	262	93.9%
	Fe	0 ppm	300	—	reference

Species	Treatment	Conc.	Count	Control	% inhibition
	Fe	1 ppm	279	300	7.0%
	Fe	10 ppm	n/a	300	n/a
	Fe	50 ppm	129	300	57.0%
	Ashwagandha	10% v/v	203	207	1.9%
	Multivitamin	10% v/v	92	207	55.6%
	Spirulina	10% v/v	225	207	−8.7%
B. megaterium (+)	Cu	0 ppm	189	—	reference
	Cu	1 ppm	116	189	38.6%
	Cu	10 ppm	16	189	91.5%
	Cu	50 ppm	10	189	94.7%
	Zn	0 ppm	206	—	reference
	Zn	1 ppm	≈83	206	59.7%
	Zn	10 ppm	11	206	94.7%
	Zn	50 ppm	11	206	94.7%
	Fe	0 ppm	187	—	reference
	Fe	1 ppm	159	187	15.0%
	Fe	10 ppm	122	187	34.8%
	Fe	50 ppm	39	187	79.1%
	Ashwagandha	10% v/v	51	218	76.6%
	Multivitamin	10% v/v	15	218	93.1%
	Spirulina	10% v/v	157	218	28.0%

Notes: EC Cu 10 ppm — unidentified white colonies observed; only morphologically typical E. coli colonies were counted. BM Zn 1 ppm — spreader adhesion smeared the plate; count is approximate. EC Fe 10 ppm — plate broken during transfer; no count available. Supplement conditions were compared to the species-matched growth control (EC: 207; BM: 218) rather than the 0 ppm metal control.

4. Discussion

4.1 Overview of Findings

Copper and zinc produced clear dose-dependent growth inhibition in both species, with *B. megaterium* consistently more sensitive than *E. coli*. Iron produced a biphasic response — stimulating or maintaining *E. coli* growth at low concentrations, then inhibiting at 50 ppm — while inhibiting *B. megaterium* across the tested range. Multivitamin extract completely suppressed *B. megaterium* but only partially inhibited *E. coli*, mirroring the metal-only pattern. Colony count data agreed with the OD-based conclusions and made it possible to quantify Spirulina, which OD could not.

4.2 Cell Wall Architecture as a Determinant of Metal Sensitivity

B. megaterium's greater metal sensitivity likely reflects cell wall architecture. The *E. coli* outer membrane restricts passive diffusion of metal ions and is backed by active efflux systems — the CopA ATPase and the CusCFBA copper efflux complex (Rensing & Grass, 2003), and the ZnuABC uptake and ZntA efflux zinc homeostasis machinery (Andrews et al., 2003; Hood & Skaar, 2012). *B. megaterium* has no outer membrane; its teichoic and lipoteichoic acids carry negative charges that bind metal ions and concentrate them at the cell surface, raising intracellular exposure. The extent of comparable homeostatic machinery in *B. megaterium* is less well characterized, which likely contributes to its lower tolerance at the concentrations tested here.

4.3 Copper-Induced Growth Inhibition

Copper inhibited both species in a dose-dependent way. In *B. megaterium*, pairwise comparisons among 1, 10, and 50 ppm were non-significant ($p_{adj} \geq 0.746$) despite declining means, so copper toxicity saturates at 1 ppm and higher concentrations cannot substantially deepen the suppression within 6 hours. *E. coli* showed a stepwise dose-response through 50 ppm, matching partial tolerance from active efflux (Rensing & Grass, 2003). Elevated copper generates reactive oxygen species and displaces iron-sulfur cluster cofactors (Imlay, 2013), mechanisms that would disproportionately hit Gram-positive commensals such as *Lactobacillus* and *Bifidobacterium* at physiologically achievable supplementation levels.

4.4 Zinc Tolerance in E. coli and Sensitivity in B. megaterium

Zinc produced the sharpest species split. *E. coli* AUC at 1 ppm equaled control ($p_{adj} = 0.991$), and a calculable growth rate persisted at 10 ppm — behavior consistent with the ZnuABC/ZntA homeostasis machinery (Andrews et al., 2003; Hood & Skaar, 2012). *B. megaterium* was already suppressed at 1 ppm ($p_{adj} = 0.007$) and completely inhibited at 10 and 50 ppm (μ = NC). Standard zinc supplements deliver 8–15 mg per serving, so 1 ppm is well inside the range that could reach the gut lumen after ingestion. This selective effect on Gram-positive gut commensals is directly relevant to how zinc supplementation is used (Huynh et al., 2022).

4.5 Iron as a Growth Stimulant at Low Concentrations

Iron produced a biphasic response in *E. coli*. Growth rates at 1 and 10 ppm Fe ($\mu = 0.802$ and $0.887\ h^{-1}$) exceeded the no-iron control ($\mu = 0.556\ h^{-1}$), which suggests the LB medium was mildly iron-limited and that supplemental iron relieved that limitation. At 50 ppm, growth was reduced and the exponential phase shifted late — a Fenton-radical picture, with hydroxyl radicals from Fe^{2+} and H_2O_2 causing oxidative damage analogous to copper toxicity at high dose (Imlay, 2013). *B. megaterium* was inhibited across the tested range, with IC_{50} between 1 and 10 ppm. This split matches clinical reports that oral iron supplementation depletes beneficial Lactobacillaceae while enriching pathogenic Enterobacteriaceae such as *E. coli* and *Salmonella* (Jaeggi et al., 2015; Paganini & Zimmermann, 2017).

4.6 Dietary Supplement Extracts and Selective Bacterial Inhibition

Ashwagandha and Multivitamin extracts both reduced bacterial AUC. Multivitamin was the clearest hit: complete suppression of *B. megaterium* (μ = NC; AUC = 0.019 ± 0.009) alongside partial inhibition of *E. coli* (AUC = 0.429 ± 0.103) — the same Gram-positive-selective pattern as Cu and Zn alone, and consistent with typical Multivitamin content (Cu 1–2 mg, Zn 8–15 mg, Fe 8–18 mg per serving). Definitive attribution to metals rather than non-metal constituents would require ICP-MS characterization of the extract (El Hosry et al., 2023). Ashwagandha showed a large OD-versus-CFU split for *E. coli*: 61% AUC reduction with only 1.9% colony count inhibition — a bacteriostatic profile, matching reported withanolide and alkaloid activity (Mishra et al., 2000). Spirulina, evaluable only by colony count because of pigment interference, gave moderate *B. megaterium* inhibition (28%) with no *E. coli* effect, extending the Gram-positive-sensitive pattern to a third supplement.

4.7 Chromophore Adsorption onto Bacterial Cell Surfaces

Raw T=0 OD_{600} in bacteria-containing cuvettes was systematically lower than in matched no-cell blanks (Multivitamin: 0.048–0.049 vs 0.070; Ashwagandha: 0.051–0.053 vs 0.063), the opposite of additive scattering. The best explanation is rapid electrostatic adsorption of cationic supplement components ($Fe^{2+/3+}$, Cu^{2+}, Zn^{2+}, riboflavin, phenolic compounds) onto the negatively charged bacterial cell surface — LPS in *E. coli*, teichoic acids in *B. megaterium* — which pulls chromophore out of the optical path within seconds of mixing (Beveridge & Murray, 1980; Vijayaraghavan & Yun, 2008). This adds a small systematic bias at early timepoints but does not affect AUC-based conclusions.

4.8 Implications for Gut Microbial Homeostasis

The gut microbiome is dominated by Gram-positive Firmicutes and Actinobacteria — including *Lactobacillus*, *Bifidobacterium*, and *Clostridium* — alongside Gram-negative Proteobacteria and Bacteroidetes (Bushman & Skaar, 2025; Huynh et al., 2022). If Gram-positive gut commensals are as sensitive to Cu, Zn, and Fe as *B. megaterium* is here, then oral supplementation at doses that reach biologically relevant intestinal concentrations could selectively deplete protective Gram-positive populations while sparing Gram-negative organisms. That kind of selective pressure could contribute to the dysbiosis and gastrointestinal symptoms often reported with high-dose mineral supplementation (Wooltorton, 2003). Pure-culture data cannot capture the full community dynamics, but they identify a mechanism worth testing in a mixed community.

4.9 Limitations and Future Directions

Several limitations apply. The 6-hour window did not capture stationary phase in the controls, so AUC reflects growth progress rather than carrying capacity. The concentration series (0, 1, 10, 50 ppm) is too coarse for reliable IC_{50} estimation. Statistical power was limited by n = 3 replicates for OD data and n = 1 for colony counts. Supplement extracts were crude water-soluble fractions; ICP-MS quantification (El Hosry et al., 2023) and follow-up with low-cost detection platforms such as ion-current-rectifying quartz nanopipettes (Farrell et al., 2024) would sharpen metal attribution. Coffee filtration does not sterilize the extract; a 0.22 µm syringe filter should be used in future runs. The broken *E. coli* Fe 10 ppm plate left the stimulatory iron effect unvalidated by plate count, and Fe precipitate scattering at 50 ppm made the OD-AUC estimate of inhibition (87%) higher than the plate-based estimate (57%). Future work should extend the model to gut-relevant species (*Lactobacillus acidophilus*, *Bifidobacterium longum*, *Bacteroides fragilis*) and to co-culture competition assays where Gram-positive and Gram-negative organisms share a metal-loaded environment.

5. Conclusion

Trace metals at concentrations relevant to dietary supplement use differentially inhibit Gram-positive and Gram-negative bacteria, with the Gram-positive *B. megaterium* consistently more sensitive than the Gram-negative *E. coli* across copper, zinc, and iron. Copper and zinc drove dose-dependent inhibition in both species, and *B. megaterium* reached complete suppression at concentrations where *E. coli* retained measurable growth. Iron produced a biphasic response in *E. coli*, with growth stimulation at 1 and 10 ppm and inhibition at 50 ppm; *B. megaterium* was inhibited across the range. The differential is consistent with the outer membrane and efflux systems that Gram-negative bacteria have and Gram-positive bacteria lack. Colony count data corroborated the OD-based conclusions and added three insights: Ashwagandha activity against *E. coli* is bacteriostatic rather than bactericidal, Spirulina inhibits *B. megaterium* moderately (28%) without touching *E. coli*, and Fe 50 ppm inhibition is less severe than OD alone suggested.

The supplement extracts recapitulated the metal-only patterns. Multivitamin completely suppressed *B. megaterium* while only partially inhibiting *E. coli*; Ashwagandha partially inhibited both species and extended the lag phase in both. Spirulina could not be scored by OD because of pigment interference, which is a real methodological ceiling for highly pigmented botanical extracts and argues for CFU-based or alternative-wavelength readouts in those cases.

The results support the hypothesis that supplement-derived trace metals can selectively reduce Gram-positive commensals while sparing more resistant Gram-negative organisms. If this pressure operates in the complex microbial community of the human gut, it could feed the dysbiosis, loss of diversity, and gastrointestinal symptoms reported with high-dose mineral supplementation. The model system used here is simpler than the gut environment, but it is controlled and reproducible, and it flags a follow-up worth doing in more physiologically representative systems. Dose and pre-existing microbial composition warrant more careful thought when evaluating the safety of trace metal supplementation, especially in people with established gut dysbiosis or low microbial diversity.

References

[1] Andrews SC, Robinson AK, Rodríguez-Quiñones F. Bacterial iron homeostasis. FEMS Microbiol Rev. 2003 Jun;27(2–3):215–237. doi:10.1016/S0168-6445(03)00055-X.

[2] Beveridge TJ, Murray RGE. Sites of metal deposition in the cell wall of *Bacillus subtilis*. J Bacteriol. 1980 Feb;141(2):876–887. doi:10.1128/jb.141.2.876-887.1980.

[3] Bushman SD, Skaar EP. The exploitation of nutrient metals by bacteria for survival and infection in the gut. PLoS Pathog. 2025 Oct 30;21(10):e1013580. doi:10.1371/journal.ppat.1013580.

[4] El Hosry L, Sok N, Richa R, Al Mashtoub L, Cayot P, Bou-Maroun E. Sample preparation and analytical techniques in the determination of trace elements in food: a review. Foods. 2023 Feb 20;12(4):895. doi:10.3390/foods12040895.

[5] Farrell EB, McNeill F, Weiss A, Duleba D, Guiry PJ, Johnson RP. The detection of trace metal contaminants in organic products using ion current rectifying quartz nanopipettes. Anal Chem. 2024 Apr 16;96(15):6055–6064. doi:10.1021/acs.analchem.4c00634.

[6] Hood MI, Skaar EP. Nutritional immunity: transition metals at the pathogen-host interface. Nat Rev Microbiol. 2012 Aug;10(8):525–537. doi:10.1038/nrmicro2836.

[7] Huynh U, Qiao M, King J, Trinh B, Valdez J, Haq M, Zastrow ML. Differential effects of transition metals on growth and metal uptake for two distinct *Lactobacillus* species. Microbiol Spectr. 2022 Feb 23;10(1):e0100621. doi:10.1128/spectrum.01006-21.

[8] Imlay JA. The molecular mechanisms and physiological consequences of oxidative stress: lessons from a model bacterium. Nat Rev Microbiol. 2013 Jul;11(7):443–454. doi:10.1038/nrmicro3032.

[9] Jaeggi T, Kortman GAM, Moretti D, Chassard C, Holding P, Dostal A, et al. Iron fortification adversely affects the gut microbiome, increases pathogen abundance and induces intestinal inflammation in Kenyan infants. Gut. 2015 May;64(5):731–742. doi:10.1136/gutjnl-2014-307720.

[10] Mishra LC, Singh BB, Dagenais S. Scientific basis for the therapeutic use of *Withania somnifera* (Ashwagandha): a review. Altern Med Rev. 2000 Aug;5(4):334–346.

[11] Paganini D, Zimmermann MB. The effects of iron fortification and supplementation on the gut microbiome and diarrhea in infants and children: a review. Am J Clin Nutr. 2017 Dec;106(Suppl 6):1688S–1693S. doi:10.3945/ajcn.117.156067.

[12] Rensing C, Grass G. *Escherichia coli* mechanisms of copper homeostasis in a changing environment. FEMS Microbiol Rev. 2003 Jun;27(2–3):197–213. doi:10.1016/S0168-6445(03)00049-4.

[13] Silhavy TJ, Kahne D, Walker S. The bacterial cell envelope. Cold Spring Harb Perspect Biol. 2010 May;2(5):a000414. doi:10.1101/cshperspect.a000414.

[14] Vijayaraghavan K, Yun YS. Bacterial biosorbents and biosorption. Biotechnol Adv. 2008 May–Jun;26(3):266–291. doi:10.1016/j.biotechadv.2008.02.002.

[15] Wooltorton E. Too much of a good thing? Toxic effects of vitamin and mineral supplements. CMAJ. 2003 Jul 8;169(1):47–48.